Itinerant antiferromagnetism in the nearly-heavy-fermion compound $NpSn_3$

M. R. Norman and D. D. Koelling
Materials Science and Technology Division, Argonne National Laboratory, Argonne, Illinois 60439
(Received 25 October 1985)

$NpSn_3$, with a paramagnetic electronic specific-heat coefficient γ, of 242 mJ/mol K^2, undergoes an antiferromagnetic phase transition at 9.5 K with a resultant drop in γ to 88 mJ/mol K^2. This behavior of γ (reduction by 64%) is typical of the "heavier" fermion antiferromagnets U_2Zn_{17}, UCd_{11}, and $CePb_3$. Self-consistent linear-augmented-plane-wave calculations within the local-density approximation have been performed for both phases to study this effect. The calculations include both spin-orbit and magnetic coupling on the same level throughout the self-consistency process. An electronic specific-heat coefficient of 102 mJ/mol K^2 is found for the paramagnetic phase—the largest value ever reported from a band-structure calculation. This large value implies that large enhancements observed in other heavy-fermion materials are not present in $NpSn_3$. A specific-heat coefficient of 39.7 mJ/mol K^2 was found for the antiferromagnetic phase, yielding a calculated 61% reduction in γ as a consequence of undergoing the phase transition. A total moment of $0.21\mu_B$ was obtained (-0.18 spin, 0.39 orbital) indicating the itinerant nature of the magnetism. An analysis of the dramatic reduction in electronic specific heat through the transition, as well as the temperature dependence of C/T in the paramagnetic phase, is presented along with a discussion of the implications for the other heavy-fermion antiferromagnets.

I. INTRODUCTION

There is much recent interest in the electronic properties of the so-called heavy-fermion compounds—those compounds which possess abnormally large electronic specific heats (for a good review, see Ref. 1). Most attention has been focused on the superconducting compounds, while relatively little attention has been given to the compounds which order antiferromagnetically. The first example of this latter class to be discovered was $NpSn_3$.[2] This compound exhibits an electronic specific-heat coefficient γ of 242 mJ/mol K^2 in the paramagnetic phase above an antiferromagnetic phase transition which occurs at 9.5 K. This transition to an antiferromagnetic phase results in a reduction of γ to 88 mJ/mol K^2 (a 64% drop). More recently, similar behavior has been found for several compounds with much larger values for γ such as U_2Z_{17} (Ref. 3) (63% reduction) and UCd_{11} (Ref. 4) (70% reduction). Trainor *et al.*[2] initially observed that the specific-heat curve for $NpSn_3$ agreed with predictions for itinerant electron antiferromagnets[5] and this was further supported by the low hyperfine field found for $NpSn_3$. Using a correlation for Np compounds of Dunlap and Lander[6] between hyperfine field and ordered moment, a moment value of $0.28\mu_B$ was suggested.[2] This value is suspect, however, because the correlation utilized was derived from Np compounds with a localized moment. Still, the resulting very low value indicates an itinerant nature of the moment. The hyperfine structure also indicates that one of the Sn sites is polarized while the other two are not.[2] The simplest assumption exhibiting these properties is that all Np moments in (001) planes order in the same direction with the stacking of alternately ordered planes. It would be reasonable to assume that this is related to a generalized Jahn-Teller-like distortion where the transformation to the antiferromagnetic state is the symmetry-lowering transformation that splits the high density of states at the Fermi energy (analogous to the degenerate highest occupied level of the molecular problem). This should be energetically favorable as it has previously been found[7] that the Stoner criterion is much exceeded with $IN(E_F)\sim 8.5$. In the configuration assumed for $NpSn_3$, the magnetic unit cell is now twice the paramagnetic unit cell with the corresponding reduction of the Brillouin zone by a factor of 2. Figure 1 shows this, assuming the configuration we will utilize: alternating planes of polarization along the z axis.

The essence of the Jahn-Teller effect is that given a degeneracy at the Fermi energy, the system can lower its (total) energy by undergoing a symmetry-breaking transition since it is of necessity the occupied levels that will move down in energy, and it costs no energy in the ground state to move up the unoccupied levels. This effect makes it difficult to explain how heavy-fermion systems like $CeAl_3$ could be stable if the driving mechanism is only that of the existence of a narrow band at the Fermi energy. Our working hypothesis has been that the localization of the f orbitals produces a narrow band,[8] but that this is only a small part of the observed effect, the remainder arising from the enhancement effects of many additional low-lying excitations. However, the antiferromagnetic materials behave more normally by actually undergoing a symmetry-lowering transition and should be more amenable to a standard band-structure calculation.

There is another difficulty that occurs when one considers the actual application. To test the assumed hypothesis, it is necessary to perform calculations with full lattice symmetry both before and after the transition. Today, this necessitates utilizing a density-functional formulation of the problem within the local-density approxima-

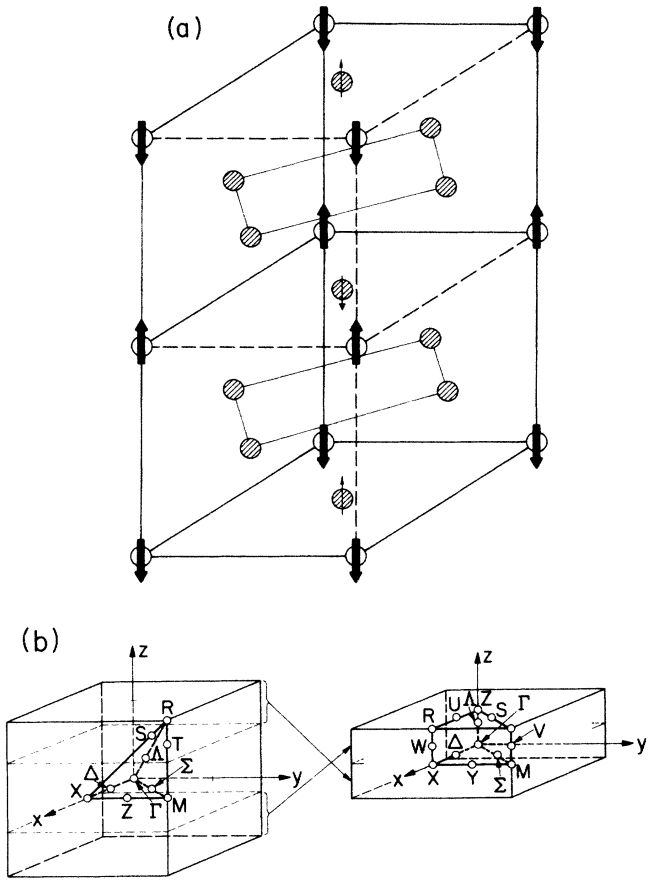

FIG. 1. (a) Assumed unit-cell geometry for the antiferromagnetic state and (b) resultant modification of the Brillouin zone. $NpSn_3$ is a Cu_3Au structure which is based on a fcc lattice with the Sn (shown as crosshatched circles) occupying the face-centered sites and the Np (open circles) occupying the corner sites. The magnetic structure doubles the unit-cell dimension in the z direction, forming alternately polarized layers of Np (with Sn weakly and oppositely polarized in the plane) separated by unpolarized Sn layers. This reduces the size of the Brillouin zone as shown with the two individual points of the simple-cubic zone differing by $(0,0,\pi/a)$ being mapped into the same point in the reduced zone. The antiferromagnetic structure is then affected by a mixing of the wave functions from these two points as described in the text.

tion (LDA). It is well known that the local-density approximation begins to break down with increasing localization. This is primarily due to the replacement of the Fock exchange operator by a local operator (Coulomb correlations are present within the LDA in an average sense). Still, the range of validity of the LDA is much larger than one would expect, and in fact does not do too badly even for free atoms. One of the best examples of this is the case of mixed valent $CeSn_3$ ($\gamma=73$ mJ/mol K^2) (Ref. 9), which has the same structure as $NpSn_3$. Thermodynamic data for $CeSn_3$ seem to be in good agreement for those predicted of a Kondo metal,[10] yet the Fermi surface predicted from a LDA calculation[11] agrees well with de Haas–van Alphen data.[12] Such agreement is not by chance since the Fermi surface topology is different from that of isostructural $LaSn_3$. $CeSn_3$ is actually an example of a strongly exchange-enhanced compound since the cyclotron masses are about a factor of 6 larger than the band masses. This is thought to be due to spin fluctuation effects[7] which are not included in the ground-state calculation. Such spin-fluctuation effects, though, can be expressed with a density-functional formalism,[13] but unfortunately the resulting equations are very computationally intensive. How far this approach would go in explaining the discrepancies between experiment and LDA band masses for heavy-fermion compounds is still unknown. The point to be gained is that the LDA appears to be giving a good description for the f electrons in the ground state of $CeSn_3$, at least in an average sense, even though thermal effects are not fully described by the standard procedure. This leads to some hope that the LDA will be adequate for those compounds where γ is not too high. Clearly, one has greater hope that such is the case for $NpSn_3$ than for the higher γ compounds like U_2Zn_{17} and UCd_{11}.

In the next section the calculational techniques used are presented. These are dealt with in a cursory fashion except where we are extending common practice. In Sec. III the results are presented and analyzed. Some care has been taken to analyze the temperature dependences and it is found that the simplest model of "fixed" band sampled by a broadening Fermi occupation factor works well for $NpSn_3$. Finally, we offer a somewhat more speculative discussion of the results in Sec. IV.

II. CALCULATIONAL PROCEDURE

Previous band-structure calculations on the paramagnetic phase of $NpSn_3$ (as well as $CeSn_3$ and USn_3) have been briefly discussed.[7] The method employed is the self-consistent warped-muffin-tin-linear-augmented-plane-wave technique. (By warped muffin tin, we mean that the potential is spherically averaged within the muffin tins but allowed to have a general shape in the interstitial region.) Such an approximation works well for these Cu_3Au structured compounds since the rare earth or actinide is at a site of cubic symmetry where nonspherical terms start at $l=4$ and the tins are at sites of D_{4h} symmetry where $l=2$ also enters. The tin bands are quite broad and dominated at the Fermi energy by their interaction with the f electrons. As mentioned above, the local-density approximation is used. We employ the exchange-correlation (XC) potential of von Barth and Hedin.[14] The choice of XC potential is not crucial since the direct Coulomb interactions with the f orbitals dominate.[7]

Although very delicate and tedious because of the sensitivity implied by the very narrow features in the density of states at the Fermi energy, the paramagnetic case is otherwise straightforward and is considered first. $NpSn_3$ crystallizes in the Cu_3Au structure with a simple-cubic Brillouin zone (Fig. 1). We use a lattice constant of 8.74 a.u. with equal muffin-tin radii for the Np and Sn sites. The number of plane-wave basis functions in the intersti-

tial region was chosen to make the muffin-tin radius times the longest reciprocal vector equal to 8.3. This results in 203 basis functions at the zone center (this number is typical, although it is larger for other points in the zone). A grid of 56 points ($\pi/5a$ mesh) in the irreducible wedge ($\frac{1}{48}$th) of the zone is used during the self-consistently process of the paramagnetic system, a tetrahedron scheme being used to find the Fermi energy and weighting. At the conclusion of the self-consistent-field (SCF) calculation, eigenvalues at an additional 99 points (the centers of 64 tetrahedron and 35 extra points from a displaced grid) were generated for further analysis. A Fourier-series spline fit[15] utilizing 331 star functions is then obtained on the full 155 points. This fit is constrained to pass through all data points and the remaining coefficients obtained from conditions of smoothness. The fit is then used to generate a density of states (DOS) utilizing 4096 tetrahedra in the irreducible wedge.

The question of relativistic effects is very important for actinide compounds and merits some discussion. A standard technique used is to perform a scalar relativistic SCF calculation[16] (i.e., ignore spin-orbit effects) and then include spin orbit via a second variational step[15] only after the SCF calculation. Our experience has been that this does not work well for many actinide materials because it does not keep the strong Coulomb interactions in balance that are, in many cases, pinning a peak in the density of states to the Fermi energy. $NpSn_3$ provides an excellent example of just such a case. This deficiency is readily repaired by moving the second variational step that includes the spin-orbit effects into the self-consistency cycle. This will work well for those materials that do not have relativistic valence p states.[17] (Note that all core states are treated as fully relativistic and nonfrozen in an overlapping core model.[18]) The advantages of this procedure are twofold: (i) computational time is reduced by about a factor of 5 over solving the full Dirac equation, and (ii) the inclusion of magnetic coupling is facilitated, as will be seen when the antiferromagnetic case is considered. Because we have also been performing fully relativistic calculations, the quality of this approximation is easy to check specifically for the case of $NpSn_3$. Upon completion of the scalar relativistic plus spin-orbit SCF calculations, the resultant density and potential were put into the fully relativistic version and a self-consistency cycle performed. We observed no significant change. This was most heartening as it implies that attention can be fully turned to the antiferromagnetic case with confidence that it will not be flawed by an inadequate account of the relativistic effects.

The antiferromagnetic case presents another difficult problem. The inclusion of both spin orbit and spin effects within the same calculation is a difficult problem which is not well handled in most cases. It is here that the smallness of the moment in $NpSn_3$ can be exploited and the advantage of treating spin orbit in a second variational step now becomes clear. A basis set is first step up by solving a scalar relativistic paramagnetic problem with the average potential (i.e., omitting the magnetic splittings). Next, this basis set is used in the second variational calculation[19] to include *both* the spin orbit and the magnetic effects. The approximation is, of course, that the spin-orbit matrix elements are determined using the average momentless potential rather than the actual one. This is definitely a second-order effect and, in light of the small moment, its omission is an excellent approximation. We assume that the moments point along one of the cubic axes with the direction alternating for successive (001) planes, as implied by the Mössbauer data,[2] as shown in Fig 1. We also assume a minimal lowering of symmetry by placing the spin polarization along the z direction. This could be determined by calculation, but as the major effect is the reduction of symmetry by the q vector, it is not appropriate at this time. The reduced symmetry of the spin-dependent potential couples states differing by $(0,0,\pi/a)$, which affects the folding of the larger cubic Brillouin zone into the smaller tetragonal zone. It is precisely the coupling of these different (in the cubic zone) $\mathbf{k}$ vectors that provides the mechanism for the wave function in the antiferromagnetic state to have different amplitudes on the two magnetically inequivalent sites. The new basis set is twice as large as for the paramagnetic case since one has not only the scalar relativistic wave functions with spin up and spin down as basis functions, but also the same set for the coupled $\mathbf{k}$ vector. The secular matrix then has the form

$$\begin{bmatrix} (E_{11}+H_{11}^{\uparrow\uparrow}+V_{11}^{a}) & V_{12}^{b} & H_{11}^{\uparrow\downarrow} & 0 \\ V_{21}^{b} & (E_{22}+H_{22}^{\uparrow\uparrow}+V_{22}^{a}) & 0 & H_{22}^{\uparrow\downarrow} \\ -H_{11}^{\uparrow\downarrow *} & 0 & (E_{11}+H_{11}^{\uparrow\uparrow *}+V_{11}^{a}) & -V_{12}^{b} \\ 0 & -H_{22}^{\uparrow\downarrow *} & -V_{21}^{b} & (E_{22}+H_{22}^{\uparrow\uparrow *}+V_{22}^{a}) \end{bmatrix},$$

where the matrix has been written in terms of matrices whose sizes are determined by the number of bands used at each of the two k points to set up the second variation. E_{ii} are the diagonal matrices of the eigenvalues of the scalar relativistic paramagnetic problem solved to determine the basis set. $H_{ii}^{\uparrow\uparrow}$ and $H_{ii}^{\uparrow\downarrow}$ are the matrices of spin-orbit matrix elements[17] and $V_{ii}^{a}=(\Delta V_{ii}^{\uparrow}+\Delta V_{ii}^{\downarrow})/2$ and $V_{ij}^{b}=(\Delta V_{ij}^{\uparrow}-\Delta V_{ij}^{\downarrow})/2$. $\Delta V^{\uparrow}(\Delta V^{\downarrow})$ is the difference between the local spin-density exchange-correlation up (down) spin potential and the unpolarized LDA XC potential. The numerical index (1 or 2) refers to the choice of the two contributing k points of the cubic cell. The basis set is

orthonormal, so one need not deal with the generalized eigenvalue problem, but merely a diagonalization. The scalar relativistic problem was solved on a $\pi/4a$ cubic mesh (35 inequivalent points). Performing the appropriate rotations, it was thus possible to set up the required pairs of k points for the $\pi/4a$ mesh in the tetragonal lattice. In this case, although the zone was shorter in the z direction, the loss of symmetry resulted in the mesh having 45 inequivalent points in the irreducible ($\frac{1}{16}$th) wedge.

The resulting second variational eigenvectors are then input into the density-potential part of the cycle. The individual spin densities are then calculated to determine $V^{\uparrow}$ and $V^{\downarrow}$. This is easily done, as the scalar relativistic wave functions used to form the basis set possess a definite spin. The problem separates nicely since the cubic k diagonal part only contributes to the cubically symmetric density and not at all to the magnetization density. This can be exploited to simplify the construction of the density. As a final step in the preparation for the next cycle, the tin densities are averaged in a two-to-one ratio to determine a cubic potential for the scalar relativistic calculation (the densities on the "magnetic" and "nonmagnetic" tin sites do not differ much).

The spin and orbital moments were calculated throughout the self-consistency process. These moments were a sensitive test of the convergence since they were the least stable property of the system. It thus took a large number of self-consistent iterations to converge both moments properly. Because the basis functions have a definite spin, the spin moment is easily calculated and requires no special comment. The orbital moment is a difficult problem that requires some attention. A full treatment of the orbital moment induced through the spin-orbit coupling should include the zone surface terms discussed in the context of susceptibility calculations.[20] However, as the major contribution is from the Np f orbitals and these are almost completely contained inside the muffin-tin spheres, it is a good approximation to use a linear-combination of atomic orbitals (LCAO)-like formalism with the atomic orbitals replaced by the radial functions of the solid.[20] Brooks and Kelley[21] have used this approximation very successfully for UN with the slight improvement that they extend out to an atomic sphere (Wigner-Seitz) radius. It is quite encouraging for our analysis of $NpSn_3$ that they obtain excellent results for UN which has a moment at least three times that of $NpSn_3$.

Upon the completion of the self-consistency process, results were obtained at an additional 90 inequivalent points. A Fourier-series spline fit was then obtained for the resulting 135-point data set using a total of 396 star functions. The density of states was obtained using the linear tetrahedron method breaking the irreducible ($\frac{1}{16}$th) wedge into 6144 tetrahedra.

III. RESULTS

In Figs. 2 and 3 the bands and density of states are shown for paramagnetic $NpSn_3$ in the vicinity of the Fermi energy (E_F). Three bands (8, 9, and 10) are seen to be virtually degenerate very near E_F over a large part of the zone. This results in a huge, narrow DOS peak at E_F corresponding to a bare band electronic specific-heat coefficient of 101.6 mJ/mol K^2, making it the largest ever reported from a band-structure calculation. The numerical reliability of such a value may be questioned. To test the sensitivity of the self-consistent process to the presence of such a narrow peak, we reconverged the calculation of Ref. 7 with a finer (by a factor of 4) energy grid for the DOS in the self-consistent code and obtained no change. When comparing spline fits involving 120 points as opposed to 155 points, we determined that the change in the γ value was less than 1%, indicating the level of sensitivity to the Fourier-spline-fit procedure. Thus, the result would appear to be reasonably precise within the framework of our particular calculation.

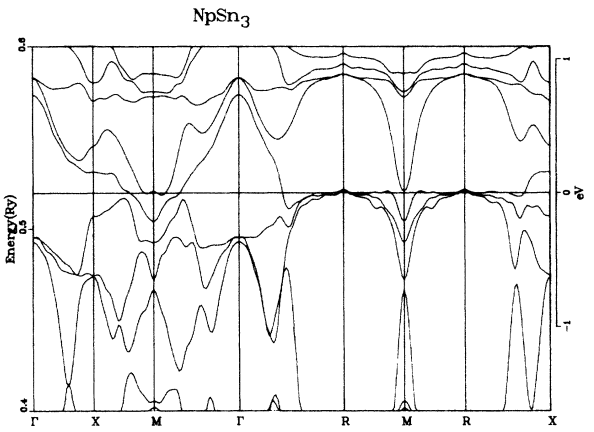

FIG. 2. Energy bands near the Fermi energy for $NpSn_3$ in the paramagnetic state. The small waves in the bands are caused by the finite spacing of the plot mesh as well as the nature of the spinning procedure.

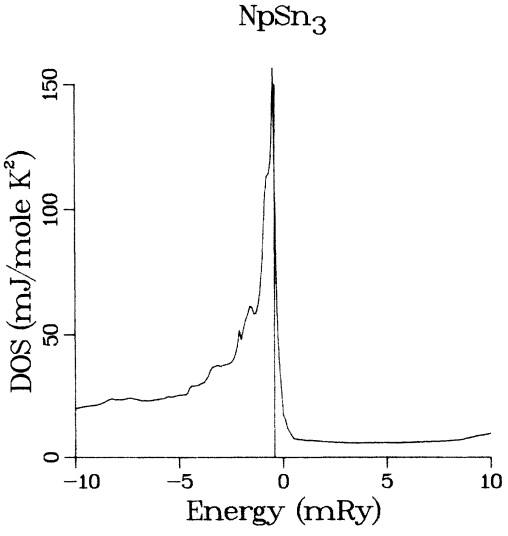

FIG. 3. Density of states near the Fermi energy for $NpSn_3$ in the paramagnetic state.

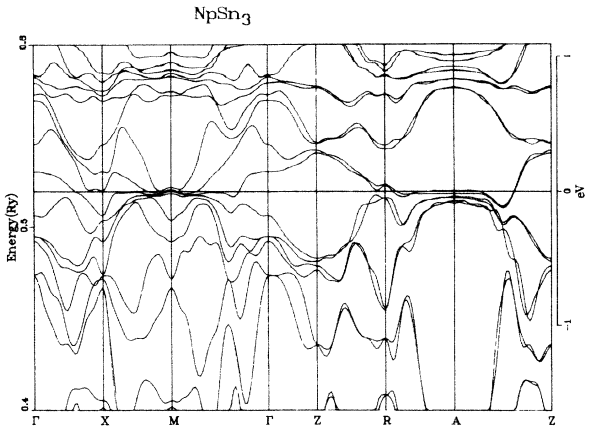

FIG. 4. Energy bands near the Fermi energy for $NpSn_3$ in the antiferromagnetic state.

The bands and density of states for the antiferromagnetic case are shown in Figs. 4 and 5. The density of states at the Fermi energy yields a bare band electronic specific-heat coefficient of 39.7 mJ/mol K^2. This is a 61% reduction of γ through the phase transition, in rather amazing agreement with the experimental value of 64%.

The origin of this reduction becomes clear from an examination of the bands in the vicinity of the Fermi energy. In the paramagnetic phase, three nearly degenerate bands (8,9, and 10) cross E_F as shown in Fig. 3. Bands 8 and 9 form small hole pockets at R which contribute little to the density of states. The huge contribution is from band 10 which forms two surfaces. The first is a ball network centered at R with the balls being so large that they interpenetrate. Inside those balls is a topologically complex surface, also centered at R, which provides the main contribution to the high specific heat (its exact structure could not be determined because of the high masses involved). In the antiferromagnetic phase, each of the previous paramagnetic bands splits into two. As can be seen in Fig. 5, the four bands which correspond to paramagnetic bands 8 and 9 have been pushed below the Fermi energy. More importantly, the two bands arising from band 10 have split, with the lower one being pushed down so that the only part of the Fermi surface it forms is a similar ball network as before, but centered at M this time (i.e., it is a fold back of the paramagnetic surface). The large-mass part of this band has been pushed below the Fermi energy. The upper band still forms two surfaces, a ball network centered at A (tetragonal A is halfway between M and cubic R) interconnected by short tubes this time, and a large-mass complicated surface running between M and A, this being the dominant contribution to the bare band electronic specific heat. This is clearly the mechanism described in the introduction as a generalized Jahn-Teller-type distortion.

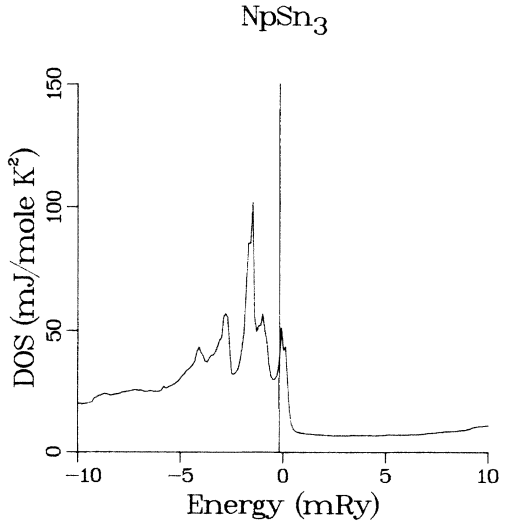

FIG. 5. Density of states near the Fermi energy for $NpSn_3$ in the antiferromagnetic state.

The antiferromagnetic calculation yielded a total moment of $0.212\mu_B$ on the Np site (with $0.391\mu_B$ for the orbital contribution and -0.179 for the spin) which came almost exclusively from the f orbitals. These moments were determined using the Fermi energy from the 135-point spline fit, the moment being extremely sensitive to the location of the Fermi energy. The magnetic Sn sites in the (001) plane had a moment of $-0.005\mu_B$ (the nonmagnetic Sn-site moments were over an order of magnitude smaller). The experimental value for the total moment is $0.28\mu_B$,[2] a bit higher than what is predicted here, but as mentioned in the Introduction, that value is found by extrapolating from a correlation found by Dunlap and Lander[6] between the hyperfine field and ordered moment for local-moment Np compounds. The significant result at present is that a small antiferromagnetic moment (within 25% of experiment) is predicted by the itinerant calculation. This is accomplished while maintaining a delicate charge balance: Precisely 3.92 electron charges of f character are found within the muffin-tin sphere of radius 3.08 a.u. in both the paramagnetic and the antiferromagnetic calculations. Clearly the direct Coulomb interactions are very dominant in this material with the magnetic distortion serving as only a very weak perturbation.

A discussion of the temperature dependence of the specific heat is very instructive. The data of Ref. 2 indicate that the electronic specific heat $\gamma = C_e/T$ is constant above the transition. This is in sharp contradiction to the band-structure calculation which shows that C_e/T drops dramatically with temperature. The experimental evaluation of C_e/T was obtained by subtracting off the phonon specific heat for isostructural USn_3, with the USn_3 phonon specific heat obtained by subtracting the zero-temperature γ value (171 mJ/mol K^2) from the total C/T, assuming that C_e/T is constant. Bader and co-workers[22] however, have shown that C_e/T actually drops dramatically from 171 to ~ 20 mJ/mol K^2 by ~ 80 K. (Parenthetically, the band-structure calculation for USn_3 indicates the C_e/T is practically constant and is actually equal to 22 mJ/mol K^2. This indicates that the enhancement factor, presumably due to spin fluctuations, is

strongly temperature dependent. Since the area under the experimental C_e/T curve, after subtracting off the 20-mJ/mol K^2 background, is $\sim R \ln 2$, the assumed spin fluctuations must be local in nature.) Based on these observations, it is clear that the phonon subtraction used for $NpSn_3$ needs to be reconsidered. To do this, a reference material that has an approximately constant C_e/T is needed and this is provided by UGe_3.[22] The phonon specific heat can be expressed by a temperature-dependent Debye temperature. When this is done, the resulting functional form of Θ for UGe_3 (Ref. 22) is similar to those found for other compounds[23] in that it drops from $T=0$ to a minimum at $\sim 0.1 T/\Theta_\infty$ and then rises to Θ_∞ and stays flat (Θ_∞ is determined from the high-temperature specific heat). Note that this phonon specific heat implicitly includes electron-phonon effects. To obtain the value for USn_3, the UGe_3 curve is scaled by the ratio of the two Θ_∞ values. The resulting phonon specific heat is larger than the total C at intermediate temperatures. If the dip in the Debye-temperature curve is appropriately narrowed, however, and the resulting phonon heat subtracted from the USn_3 specific-heat curve, the resulting C_e/T curve varies smoothly from 171 to 20 as T is increased. The phonon specific-heat curve thus obtained is now subtracted from the experimental C/T curve for $NpSn_3$ (Ref. 2) in the range of 3—30 K. This result is shown in Fig. 6, along with the results from the band-structure calculation. The latter was normalized by the ratio of the experimental and theoretical specific heats in the antiferromagnetic phase at $T=0$. The agreement between the two is striking (the upturn in the experimental curve at ~ 15 K marks the onset of the phase transition which is presumably broadened by fluctuations). The important point to be garnered here is that there is now a strong temperature dependence of the experimental C_e/T curve which is in essential agreement with the band-structure results.

One learns far less from the temperature dependence of the susceptibility. The temperature dependence of the susceptibility for $NpSn_3$ is shown in Ref. 24. Basically, the value is ~ 0.0016 emu/mol near $T=0$, rises to a maximum of 0.0020 emu/mol at ~ 18 K, and then slowly decreases with temperature. The susceptibility is anomalously low and also has a weak temperature dependence. The band *spin* susceptibility can be written in the local-spin-density approximation (LSDA) as[25]

$$\chi(T)=\chi_0(T)/[1-I_{XC}N(T)] ,$$

where

$$N(T)=-\int \frac{df}{de}N(e)de$$

and f is the Fermi function. I_{XC} is a Fermi surface average of the spin-spin response function in the LSDA. The LSDA estimate for χ in $NpSn_3$ is predicted to diverge up to 100 K. If one adjusts I_{XC} to match χ with the experimental value at 20 K, the resulting I_{XC} is over an order of magnitude smaller than the LSDA estimate. Moreover, the temperature dependence of even the bare theoretical χ is more rapid than the experimental dependence. Clearly, the omission of the spin-orbit interaction implied in the

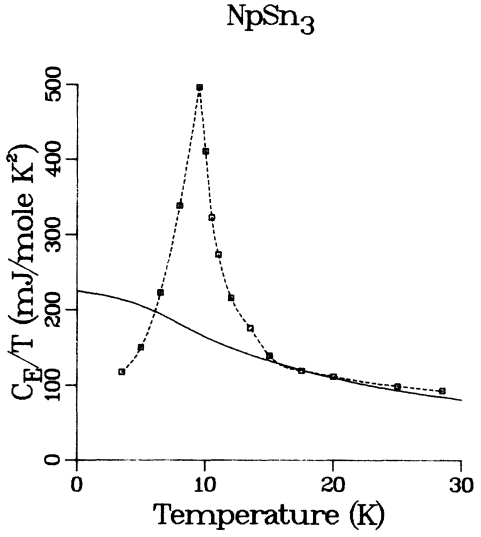

FIG. 6. Temperature dependence of the experimental (dashed curve) and theoretical (solid curve) paramagnetic electronic specific-heat coefficients C_e/T. The former was obtained as described in the text. The upturn at ~ 15 K in the experimental curve marks the onset of the transition (which is broadened by fluctuations). The theoretical curve was normalized by a ratio equal to the ratio of the experimental and theoretical specific heats in the antiferromagnetic phase at $T=0$.

utilization of the LSDA formalism is a serious limitation since the f orbitals are more nearly j states than ls states. The orbital moment is larger than, and opposed to, the spin moment so that the LSDA is not directly applicable to this situation, and a formal theory is not available for the case with orbital effects.

IV. DISCUSSION

Two observations appear crucial to ascertaining the nature of the f states in $NpSn_3$: (i) the f charge is identical in both the paramagnetic and the antiferromagnetic states, and (ii) the implied enhancements are quite modest and very nearly the same in the two states. From these observations one can assert that the direct Coulomb interaction is the dominant interaction—which is no great surprise; that the nature of the f states has not changed in going through the transition, and that there are no large dynamic effects occurring. The phase transition is not "exotic" but involves a simple Jahn-Teller-like distortion to lower the energy of the system. This is in contrast to other XSn_3 materials such as $CeSn_3$ (enhancement of 4.5—4.9) and USn_3 (enhancement of ~ 6.5) where large enhancements are observed.[7] The crucial difference is most likely that the large density of unoccupied f states found just above the Fermi energy in $CeSn_3$ and USn_3 (Ref. 7) has been pulled below the Fermi energy in $NpSn_3$ such that the phase space available for spin-fluctuation scattering is greatly reduced. This would cause a reduction in the mass enhancements as seen in Pd.[26] Further evidence that the electronic structure is not behaving in an exotic fashion is the simple behavior of the electronic contribution to the

specific heat. The temperature dependence of the electronic specific heat is well described by the effect of the thermal width of the Fermi occupation factor. The electron-phonon enhancement is small and there is no need to assume dehybridization or spin-fluctuation enhancements in this case. (Though the rise in C_e/T between 15—10 K could be due to spin fluctuations.) The magnetic response is complicated by the strength of the spin-orbit coupling for the f orbitals such that much less can be said from further analysis of that data.

Based on this discussion, we can offer some speculations concerning the nature of the heavier antiferromagnets such as U_2Zn_{17}, UCd_{11}, and $CePb_3$. The similarity of the thermodynamic data for these compounds to that for $NpSn_3$ (Ref. 1) suggests that the mechanisms discussed above occur also in these compounds. In other words, when the temperature is low enough, it is energetically favorable for the system to lower its free energy and rid itself of the high density of states at the chemical potential by undergoing a symmetry-lowering transition. Since the resulting magnetic perturbation is small, the moment is small, but the small splitting is sufficient to cause the large reduction seen in the electronic specific heat. The sensitivity of such a magnetic state has recently been dramatically demonstrated by Willis *et al.*[27] who have shown that 2% Cu substitution for Zn in U_2Zn_{17} will destroy the magnetism. This is consistent with a coherent state caused by a weak magnetic perturbation being destroyed by hybridization disruption. These arguments are quite general and independent of whether the local-density approximation works or not for these compounds.

ACKNOWLEDGMENTS

The authors would like to thank Dr. B. Dunlap for a helpful discussion on the magnetic structure. They would also like to thank Professor L. deLong for a discussion on the Wilson ratios, Dr. M. B. Brodsky, and H. Sowers for a discussion on the $NpSn_3$ data, and especially Dr. S. Bader for discussions about the phonon specific heat for USn_3. This work was supported by the U.S. Department of Energy, Office for Energy Research, Office of Basic Energy Sciences, Division of Materials Sciences, under Contract No. W-31-109-Eng-38, and a grant of computer time at the Energy Research Cray X-MP computer at the Magnetic Fusion Energy Computing Center.

[1]G. R. Stewart, Rev. Mod. Phys. **56**, 755 (1984).
[2]R. J. Trainor, M. B. Brodsky, B. D. Dunlap, and G. K. Shenoy, Phys. Rev. Lett. **37**, 1511 (1976).
[3]H. R. Ott, H. Rudiger, P. Delsing, and Z. Fisk, Phys. Rev. Lett. **52**, 1551 (1984).
[4]Z. Fisk, G. R. Stewart, J. O. Willis, H. R. Ott, and F. Hulliger, Phys. Rev. B **30**, 6360 (1984).
[5]P. A. Fedders and P. C. Martin, Phys. Rev. **143**, 245 (1966).
[6]B. D. Dunlap and G. H. Lander, Phys. Rev. Lett. **33**, 1046 (1974).
[7]M. R. Norman and D. D. Koelling, Physica **135B**, 95 (1985).
[8]D. D. Koelling, B. D. Dunlap, and G. W. Crabtree, Phys. Rev. B **31**, 4966 (1985).
[9]K. Ikeda and K. A. Gschneidner, Jr., Phys. Rev. B **25**, 4623 (1982).
[10]P. Schlottman, J. Appl. Phys. **57**, 3155 (1985).
[11]D. D. Koelling, Solid State Commun. **43**, 247 (1982).
[12]W. R. Johansen, G. W. Crabtree, A. S. Edelstein, and O. D. MacMasters, J. Magn. Magn. Mater. **31-34**, 377 (1983); W. R. Johansen, G. W. Crabtree, D. D. Koelling, A. S. Edelstein, and O. D. McMasters, J. Appl. Phys. **52**, 2134 (1981).
[13]A. H. MacDonald (private communication).
[14]U. von Barth and L. Hedin, J. Phys. C **5**, 1629 (1972).
[15]D. G. Shankland, in *Computational Methods in Band Theory*, edited by P. M. Marcus, J. Janak, and A. Williams (Plenum, New York, 1971), p. 362; D. D. Koelling and J. H. Wood, J. Comp. Phys. (to be published).
[16]B. N. Harmon and D. D. Koelling, J. Phys. C **7**, L210 (1974).
[17]A. H. MacDonald, W. E. Pickett, and D. D. Koelling, J. Phys. C **13**, 2675 (1980).
[18]D. D. Koelling, Solid State Commun. **53**, 1019 (1985).
[19]G. O. Arbman and D. D. Koelling, Phys. Scr. **5**, 273 (1972).
[20]K. H. Oh, B. N. Harmon, S. H. Liu, and S. K. Sinha, Phys. Rev. B **14**, 1283 (1976).
[21]M. S. S. Brooks and P. S. Kelly, Phys. Rev. Lett. **51**, 1708 (1983).
[22]S. D. Bader, G. S. Knapp, and H. V. Culbert, in *Magnetism and Magnetic Materials—1974 (San Fransico)*, proceedings of the 20th Annual Conference, edited by C. D. Graham, G. H. Lander, and J. J. Rhyne (AIP, New York, 1975), p. 222; M. R. Norman, S. D. Bader, and H. A. Kierstead (unpublished).
[23]G. Leibfried and W. Ludwig, in *Solid State Physics*, edited by F. Seitz and D. Turnbull (Academic, New York, 1961), Vol. 12, p. 329.
[24]M. B. Brodsky and R. J. Trainor, Physica **91B**, 271 (1977).
[25]S. H. Vosko and J. P. Perdew, Can. J. Phys. **53**, 1385 (1975); K. L. Liu, A. H. MacDonald, J. M. Daams, S. H. Vosko, and D. D. Koelling, J. Magn. Magn. Mater. **12**, 43 (1979).
[26]A. H. MacDonald, Phys. Rev. B **24**, 1130 (1981).
[27]J. O. Willis, Z. Fisk, G. R. Stewart, and H. R. Ott, J. Magn. Magn. Mater. (to be published).